Study on Mine Pressure Control by Ground Fracturing High-level Hard Rock Strata

Rui Gao (cumtgaorui@163.com)
Taiyuan University of Technology
Tiejun Kuang
Datong coal mine group
Yanqun Zhang
Datong coal mine group
Wenyang Zhang
Datong coal mine group
Chunyang Quan
Datong coal mine group

Research

Keywords: ground fracturing, high-level hard roof, breakage characteristics, pressure control, safety mining

Posted Date: September 10th, 2020

DOI: https://doi.org/10.21203/rs.3.rs-73625/v1

Version of Record: A version of this preprint was published on January 23rd, 2021. See the published version at https://doi.org/10.1007/s40789-020-00405-1.

Abstract

During extra-thick coal seam mining, the high-level thick and hard strata are the main reason for the presence of a strong ground pressure in the working face; however, there is no active and effective control technology for high-level hard strata. This paper proposes the concept of ground fracturing hard roofs, and the physical simulation was used to study the control effect of ground fracturing on the strata breaking structure and energy release. The results showed that the ground fracturing changed the structural characteristics of the strata and reduced the energy release intensity and overburden movement spatial extent, which had a significant control effect on the ground pressure. The Datong mining area was selected as the engineering background, a ground horizontal well fracturing engineering test was conducted on site, and a 20-m-thick hard rock layer, which was 110 m vertically away from the coal seam, was determined as the fracturing target layer. On-site microseismic monitoring showed that the crack propagation length was up to 216 m, and the height was up to 50 m. On-site mine pressure monitoring showed that the roadway deformation was reduced to 100 mm, the periodic weighting characteristics of the hydraulic supports were not obvious, the ground pressure in the working face was significantly controlled, and the ground fracturing was successful. Ground fracturing changed the occurrence characteristics of the high-level hard strata, which is beneficial to ameliorate the stress environment of a working face and provide a new approach of hard rock control.

Introduction

Thick and extra-thick coal seams are the main coal seams for high-efficiency mining, and presently, the caving mining method is mainly used. Owing to the large thickness of the above coal seams, the range of overburden migration is wide. Previous studies have shown that the overburden failure zone could reach more than 250 m during 14-m to 20-m-thick coal seam mining (Yu et al. 2015, 2017; Zhang et al. 2014). When there are multiple hard roofs in an overburden, the fracturing and breaking down of the hard roofs at different levels result in the frequent presence of a strong ground pressure in the stope, causing effects such as the crashing of supports and roadway damages, which seriously affect safe production (Guo et al. 2014; Yang et al. 2015; Xia et al. 2017). In view of the strong ground pressure in extra-thick coal seam mining with hard roofs, domestic and foreign scholars have conducted related research. Bin Yu (2016) studied the mechanism of strong mine pressure in Datong coal mine and pointed out that the high-level hard thick strata was the main reason causing the strong pressure in mining stope. Bednarek Lukasz (2020) discussed the rock mass characteristics which influence the choice of support. Jianguo Ning et al. analyzed the fracturing characteristics of overlying hard roofs by the method of microseismic monitoring, which could assist in explaining the strong strata behavior induced by thick and hard roofs (Ning et al. 2017, 2019). Ju Jinfeng et al. analyzed the structural characteristics of overlying hard strata and the ground pressure in a stope following a 7-m-thick coal seam mining (Ju and Xu, 2013). Jianlin Xie et al. analyzed the influence law of different thicknesses and distribution of hard roofs of the peak value and influence range of the leading abutment stress of a working face (Xia and Xu, 2017). According to a study by Li Zhu, the rotary movement of the key strata in an overburden had a direct impact on the appearance of pressure on the supports in a working face, and the influence of the rotary angle of the key strata in different levels on the stope pressure was analyzed (Li et al. 2018). Li Huamin et al. found that the large mining thickness of an extra-thick coal seam resulted in a larger mobile space of the high-level hard roofs, and this sliding instability of the high-level hard roofs induced a strong ground pressure (Li et al. 2014). Lan Yiwen et al. performed an in situ measurement method to compare the resistance distribution characteristics of the supports of the working face during extra-thick coal seam mining. The study found that the weight characteristic showed a “long duration and short duration.” When a high-level hard roof broke, the pressure strength was increased; however, there was no obvious regularity in the high-level hard strata breaking (Lan et al. 2018). Tan et al. (2018) studied the coal seam capability influenced by the overlying hard roofs. The above studies showed that during extra-thick coal seam mining, when the overburden deposits hard roofs, the large suspended area of these hard roofs was the main factor causing the strong ground pressure in the working face. Particularly the breakage and instability of the high-level hard and thick strata were identified as the main reasons for the rock mass failure and extremely high bearing stress of the coal body.

The method of active weakening is the main technical approach to reduce the breaking strength of hard roofs. At present, hydraulic fracturing and confined water-filled blasting are primarily adopted. Fracturing pumps, fracturing pipes, grooving drill bits, and other equipment are used to fracture roofs in the process of hydraulic fracturing to reduce the integrity of the roofs and achieve the goal of ground pressure control (Lu et al. 2015; Ge et al. 2015; Yu and Duan, 2014). By using a liquid explosive, the confined water-filled blasting technology can not only realize safe blasting but also improve the blasting ability to the maximum extent to reduce the breaking strength of hard roofs (Yang et al. 2017; Yang and Liu, 2017). However, constrained by the equipment, drilling length, and other conditions, the above technologies are only limited to underground operations, and the control range is within 50 m, which cannot fracture hard roofs at a high level. Therefore, the team of Prof. Yu proposed for the first time the method of ground hydraulic fracturing (Yu et al. 2019; Gao, 2018), i.e., fracturing the target roofs at a high level by drilling fracturing wells downward from the ground. In the fracturing process, only clean water was used, which was economical and environment friendly. Simultaneously, the fracturing control range was large and control effect was good.

Only a few scholars have studied the ground fracturing technology. Professor Yu proposed the method and applied it in the field for the first time, achieving an excellent control effect (Yu et al.2019). Aimed at the selection of the target layers for ground fracturing, Binwei Xia compared and analyzed the breaking strength of hard roofs at different levels and determined the reasonable range of ground fracturing layers via numerical simulation (Lu et al. 2018). Regarding the ground pressure control mechanism and influence on the strata structural morphology of ground fracturing, scholars have not conducted in-depth research. The physical similarity simulation is a research method that can accurately and intuitively reflect the structural characteristics of overburden (Yan et al. 2018). In the study, this method is used to conduct an in-depth investigation on the characteristics of the overburden displacement and strata breaking strength after ground fracturing high-level roofs to reveal the weakening mechanism of ground fracturing. A field application verification is conducted to improve the technical system of ground fracturing a high-level hard roof.

2 Proposed of ground hydraulic fracturing

2.1 Background

The #3–5 extra-thick coal seam is mainly mined in the Tashan coal mine of the Datong mining area. The coal seam thickness is 14 m to 20 m, and the method of top-coal caving mining is adopted. The coal seam is buried at a depth of 400–800 m, and there are multiple hard roofs in the overburden with a compressive strength of 60–120 MPa. In the mining process of the working face, a strong ground pressure occurs periodically, and the characteristics are mainly reflected in the following aspects:

(1) The first roof weighting pace of the working face is 46 m to 55 m. The periodic weighting of the working face is reflected in the aspects of a short and long intension period and an extremely strong intension period.

(2) Short intension period: the roof weighting step is about 12 m to 26 m, which is mainly manifested in the increase of 20 to 30 supports resistance of the working face. There is an obvious coal wall rib spalling, and the top coal can be easily caved.

(3) Long intension period: the roof weighting step is about 30 m to 52 m, the resistance of more than 40 supports of the working face increases sharply, and the safety valves are opened substantially. The coal wall rib spalling is significant, and the top coal is liable to leakage. The roadway deformation exceeds 2000 mm.

(4) Extremely strong intension period: There is no obvious weighting step, and the occurrence frequency is low. During the period, the supports on the working face are frequently crushed, the minimum size of the roadway is only 1000×1000mm, and the advanced single hydraulic props are severely bended and split.

To explore the influence of hard roofs failure and instability at different levels on the pressure appearance on a stope, a research study have been performed based on the method of field measurement (Lan et al. 2018). In this case, the thickness of the coal seam was 19 m, and the method of top-coal caving mining was adopted. The strata movement measurement points were arranged in the key strata at different levels (22, 51, and 104 m away from the coal seam). The thicknesses of the three key strata were 12, 9.8, and 23 m from the bottom up. Concurrently, the resistance characteristics of the working face supports were recorded in real time. The monitoring results showed that the support resistance in the working face increased with the breakage of two key strata that were 22 and 51 m away from the coal seam at a low level, and the dynamic load coefficient of the supports was 1.15 and 1.34, respectively. The pressure duration was 7 and 16 h, respectively, and there were no obvious indications of a strong ground pressure in the working face. When a 23-m-thick key layer (which was 104 m from the coal seam) broke, the #35–95 supports in the working face were crushed, and the dynamic load coefficient of the support reached 1.54. The pressure duration reached 43 h, and the ratio of the distance between the highest key layer and coal seam to the coal seam thickness was 5.47. It can be seen that in the mining of extra-thick coal seam, when there exists a thick and hard roof at a high level, its failure and instability will easily result in a strong impact strength, which is the main factor inducing the strong ground pressure in the working face, as shown in Fig. 1.

2.2 Technology of ground hydraulic fracturing

The presence of hard roofs at a high level is the main factor that causes the strong ground pressure in the working face. Furthermore, a large breaking step and an entire block rotation are the internal inducements of the strong ground pressure. Therefore, using a reasonable technology to weaken the hard strata in far fields and changing their physical and mechanical properties, structural occurrence, and fracture characteristics, thus reducing the breaking strength of the hard roofs and modifying the stress concentration in the stope, is an effective approach to achieve strong ground pressure prevention.

After years of research and practice, a set of hard roof control technologies based on the underground hydraulic fracturing and blasting technologies has been formed (Lu et al. 2015; Ge et al. 2015; Yu and Duan, 2014; Yang et al. 2017; Yang and Liu, 2017), which can effectively control the hard roofs at a low level from underground. However, owing to the limitations of the underground hydraulic fracturing equipment, technology, and construction conditions, it is generally only possible to weaken the hard roofs within 50 m away from the coal seam, and it is impossible to control those at a high level.

The ground drilling fracturing technology is widely used in the oil and gas exploitation process. The principle of the above technology is to manufacture cracks of a certain geometric size and conductivity artificially by a hydraulic pump. Therefore, referring to the ground fracturing technology, the team of the author innovatively proposed the concept of ground fracturing hard roofs in a coal mining area. Moreover, it used ground fracturing equipment to weaken high-level hard rock formation to reduce the integrity and strength of the hard roofs and achieve the purpose of ground pressure control (Yu et al. 2019; Gao 2018). The schematic is shown in Fig. 2.

3 Simulation study on ground pressure control by ground fracturing

In the process of ground fracturing hard roofs, in the fracturing, water is mainly used. The direction of the fracture propagation is directly related to the distribution of the three-direction stress field in rock deformation. After fracturing, the fracture distribution in the strata can be divided into three situations: (1) the formation of horizontal fracture, such that the occurrence of fracture reduces the effective thickness of the strata and the complete rock layer is divided into two or several layers; (2) the formation of vertical fracture, which cuts off the thick and hard roof into two independent structures; (3) the formation of numerous disordered fractures, which destroy the integrity of the thick and hard rock strata, dividing them into several sections. In this paper, owing to the space limitation, only the influence of vertical fracture occurrence on the characteristics of the overburden structure and ground pressure is discussed, and the occurrence of other fractures is further studied. By performing a physical similarity simulation, a vertical fracture is artificially generated in the high-level hard roof of the model. By comparison and analysis with a non-fracturing model, the structural characteristics of the overburden and variation rule of the ground pressure are studied.

3.1 Physical Model

Taking the 8101 working face in the Tashan coal mine as the reference to build the physical model, and two models are made in total. Model 1 is built according to the geological conditions, and model 2 is based on model 1 with a vertical fracture artificially created in the high-level hard roofs. Carboniferous

#3–5 coal seam is mainly mined in the 8101 working face, and the average thickness, buried depth, and inclination angle of the coal seam are 20 m, 470 m, and 1–3°, respectively. The working face length is 230 m, and the continuous mining length is about 1500 m. The coal seam is covered with multiple layers of hard roofs. The geometric size of the physical similarity model is 2.5 × 0.2 × 1.47 m (length × width × height). The similarity ratio of the model is 150:1, and the simulated laying height is 220 m.

Sand, calcium carbonate, and gypsum were used in the laboratory for modeling, and the designed bulk density ratio is 1.667:1. The motion time similarity ratio, stress similarity ratio, and dynamic similarity ratio are calculated to be 12.25:1, 250:1 and 5.63×10^{6}:1, respectively. The model is excavated continuously to the boundary every 30 min, and 5 cm is excavated each time. The thickness of the overlying unarranged rock layer is 272.65 m, and the compensation stress added to the upper part of the model is calculated to be 0.027265 MPa. The matching parameters of the rock layers obtained in the model are listed in Table 1. In Table 1, No.32, No.27, No.22, No.16, and No.9 rock formations are the key strata, which are recorded as KS1, KS2, KS3, KS4, and KS5 respectively. In this experiment, KS5 at a high level is mainly studied.

Table 1 Proportioning parameters of the rock formation

No.	Lithology	Depth/m	Thickness /m	Simulated thickness /cm	Compression strength /MPa	Simulated strength/KPa	Matching number	Weight /kg	Sand/kg	Calcium carbonate /kg	Gypsum /kg
1	gritstone	267.01	4.9	3.3	28.34	113.36	373	29.4	22.05	5.15	1.65
2	packsand	271.91	12.1	8.1	90.53	362.12	437	72.6	58.08	4.36	8.13
3	siltite	284.01	3.7	2.5	33.6	134.4	737	22.2	19.43	0.83	1.70
4	gritstone	287.71	2.8	1.9	23.1	92.4	473	16.8	13.44	2.35	0.81
5	pebblestone	290.51	4.5	3.0	35.6	142.4	555	27	22.50	2.25	1.88
6	gritstone	295.01	5	3.3	25.9	103.6	755	30	26.25	1.88	1.64
7	conglomerate	300.01	5	3.3	37.74	150.96	455	30	24.00	3.00	2.40
8	siltite	305.01	5	3.3	24.1	96.4	473	30	24.00	4.20	1.44
9	**packsand**	**310.01**	**12.9**	**8.6**	**80.21**	**320.84**	**337**	**77.4**	**58.05**	**5.81**	**10.16**
10	gritstone	322.91	5	3.3	26.6	106.4	755	30	26.25	1.88	1.64
11	medium-sandstone	327.91	4.8	3.2	30.3	121.2	655	28.8	24.69	2.06	1.76
12	siltite	332.71	3	2.0	35.87	143.48	555	18	15.00	1.50	1.25
13	conglomerate	335.71	5.2	3.5	25.6	102.4	755	31.2	27.30	1.95	1.71
14	pebblestone	340.91	5.4	3.6	32.3	129.2	737	32.4	28.35	1.22	2.48
15	siltite	346.31	4	2.7	23.57	94.28	473	24	19.20	3.36	1.15
16	**packsand**	**350.31**	**12.2**	**8.1**	**80.27**	**321.08**	**337**	**73.2**	**54.90**	**5.49**	**9.61**
17	gritstone	362.51	5.7	3.8	32.87	131.48	737	34.2	29.93	1.28	2.62
18	conglomerate	368.21	3.3	2.2	22.9	91.6	473	19.8	15.84	2.77	0.95
19	siltite	371.51	3	2.0	33.85	135.4	737	18	15.75	0.68	1.38
20	medium-sandstone	374.51	4.83	3.2	30.24	120.96	655	28.98	24.84	2.07	1.77
21	siltite	379.34	5	3.3	23.23	92.92	473	30	24.00	4.20	1.44
22	**packsand**	**384.34**	**10.12**	**6.7**	**65.53**	**262.12**	**337**	**60.72**	**45.54**	**4.55**	**7.97**
23	pebblestone	394.46	5.6	3.7	30.23	120.92	373	33.6	25.20	5.88	1.89
24	mudstone	400.06	5.8	3.9	25.3	101.2	755	34.8	30.45	2.18	1.90
25	conglomerate	405.86	3.8	2.5	29.13	116.52	373	22.8	17.10	3.99	1.28
26	siltite	409.66	5.25	3.5	36.56	146.24	555	31.5	26.25	2.63	2.19
27	**packsand**	**414.91**	**9.1**	**6.1**	**55**	**220**	**437**	**54.6**	**43.68**	**3.28**	**6.12**
28	siltite	424.01	6.4	4.3	30.73	122.92	655	38.4	32.91	2.74	2.35
29	conglomerate	430.41	3.2	2.1	23.6	94.4	473	19.2	15.36	2.69	0.92
30	medium-sandstone	433.61	4	2.7	30.43	121.72	655	24	20.57	1.71	1.47
31	gritstone	437.61	5.05	3.4	38.6	154.4	455	30.3	24.24	3.03	2.42
32	**packsand**	**442.66**	**9.44**	**6.3**	**55.53**	**222.12**	**437**	**56.64**	**45.31**	**3.40**	**6.34**
33	sandy mudstone	452.1	5.65	3.8	33.3	133.2	737	33.9	29.66	1.27	2.60
34	conglomerate	457.75	3.2	2.1	23.34	93.36	473	19.2	15.36	2.69	0.92
35	siltstone	460.95	4.4	2.9	21.07	84.28	573	26.4	22.00	3.08	1.10
36	mudstone	465.35	4.3	2.9	17.36	69.44	773	25.8	22.58	2.26	0.85
37	#3-5 coal seam	469.65	20	13.3	15.94	63.76	773	120	105.00	10.50	3.94
38	gritstone	489.65	3	2.0	43.87	175.48	637	18	15.43	0.77	1.54

In model 2, a crack is set artificially in KS5 at a position of 90 m horizontally from an open-off cut by a thin iron piece to reduce the integrity of the KS5. A prefabricated crack is formed in the model by placing a 0.2-mm-thick piece of iron in the fractured target layer. Because the model is 20 cm wide, two 10 × 10 cm thin iron sheets are used. The model and fracture setting scheme are shown in Fig. 3 (a). Fig. 3(b) shows the monitoring scheme of the overburden displacement. The Vic-2D non-contact strain monitoring system is used, black speckles are sprayed on the surface of the model, and the displacement of the overlying strata is obtained by monitoring the displacement of each scattered black point.

Result Analysis

(1) Characteristics of overburden structure after ground fracturing

The structural characteristics of the high-level KS4 and KS5 are analyzed. The structural characteristics of KS4 and KS5 before and after KS5 is fractured are shown in Fig. 4.

As shown in Figures 4(a) and (c), the high-level KS5 is not fractured, the breaking span of KS4 and KS5 are 170m and 175m respectively. The breakage of KS4 and KS5 causes an unstable and a synchronous rotation of the lower strata, and the range of the motion space in the overburden is wide. The vertical displacement of the cantilever beam structure close to the working face caused by the breakage of KS5 and KS4 is 0.48 m and 2.5 m, respectively.

After KS5 is fractured, the first breaking span of the high-level KS4 is reduced to 142 m, of which the length of the broken block A is only 47 m, and the displacement of the immediate roof at the working surface is 0.45 m, as shown in Fig. 4(b). Compared to the KS5 unfractured model, the KS4 breaking span is reduced after KS5 is fractured; this is mainly because the bearing capacity of KS5 is reduced after fracturing. Moreover, the weight of KS5 and its overlying strata is transferred to KS4, increasing the load above KS4, thus causing the breaking span to decrease. It also can be seen from Fig. 4(b) that after KS4 is broken, KS5 also undergoes a large degree of deflection and rotation by the fracturing action, but it does not rotate synchronously with KS4 and still maintains a certain structural stability.

As the working face continues mining, KS5 continues to rotate. Because of its relatively slow rotation, its breaking and unstable energy release intensities are low and have no impact on the underlying strata. The underlying key layer structure can be kept stable. The rotation of the KS5 breaking block does not generate a ground pressure, as shown in Fig. 4(d).

(2) Strata movement control effect of ground fracturing

Taking KS4 and KS5 as the research objects, their vertical displacement changes are obtained when they are broken under the conditions of occurrence and non-occurrence of KS5 fractured, as shown in Fig. 5. The abscissa is the position of the measurement point along the model mining direction.

As shown in Fig. 5(a), in the absence of KS5 fractured, when KS4 breaks, the maximum vertical displacement of KS5 is 1.2 m, and the KS5 structure remains stable. After the KS5 fractured, when KS4 breaks, the KS5 structural integrity is reduced, being affected by the weakening of the ground fracturing, and a large bending subsidence of 1.73 m occurs in KS5. However, the KS5 structure does not sink with KS4 synchronously, and it can maintain the structural stability and a certain separation space with the underlying rock formation. As the working face continues mining, KS5 slowly settles to stability.

It can be seen from Fig. 5(b) that when KS5 is not subjected to ground fracturing, its integrity is strong, and the breaking span is 175 m. The large rotary movement and high strength during KS5 breakage causes a synchronous movement of the underlying strata. Taking KS4 as an example, the KS5 breakage causes the vertical displacement of KS4 to reach 1.68 m. When KS5 is fractured, the rotation of KS5 is no longer a transient, high-speed, high-intensity movement process but a slow deflection and sinking one. The strength and energy release during the KS5 breakage is low, which has a weak impact on the underlying rock formation. The rotation of KS5 after the ground fractured will barely cause a synchronous movement of the underlying rock formation, the vertical displacement of KS4 hardly changes, and the KS4 structure remains stable. It can be seen that the ground fracturing significantly reduces the movement strength of the hard strata.

In addition, after KS5 is fractured, owing to its reduced bearing capacity, the part weight of the overburden is carried by KS4, which increases the load strength above KS4, causing the KS4 breaking span to decrease. It is found in the experiment that the KS4 breaking span reduces to 142 m, which is reduced by 28 m compared to the model of KS5 unfractured. Moreover, the degree of the strong mine pressure of KS4 breaking is reduced to a certain extent.

The vertical displacement of the immediate roof next to the supports during the breakage of KS4 and KS5 in the absence and presence of KS5 fractured is shown in Fig. 6. It can be seen from Fig. 6 that when the ground fracturing of high-level KS5 is not implemented, the breakage of KS4 results in a maximum sinking of 2.5 m in the immediate roof, which will probably cause the supports to crash on the working face. After KS5 is fractured from the ground, the vertical displacement of the immediate roof caused by the breakage of KS4 is significantly reduced to 0.45 m, and the KS5 rotation process barely causes the motion of the underlying strata. The ground fracturing of the high-level hard strata has a significant effect on reducing the strong mine pressure in the working face.

(3) Control effects of overburden movement space

The experimental research shows that the ground fracturing of high-level KS5 is beneficial for reducing the breaking span of KS5 and the low key strata, thereby reducing the influence range during the breakage of high-level thick and hard rock strata and avoiding the formation of excessive structures in the overlying large space. The degree of the strong ground pressure in the working face is reduced, and the spatial structure of the overlying rock before and after KS5 fractured are shown in Fig. 7.

It can be seen from Figures 7(a) and (c) that when KS5 is not fractured, the large structural dimensions in the overburden after high-level key layers KS4 and KS5 break are 210 × 165 m and 225 × 165 m respectively, and after KS5 is fractured, the structural size is reduced to 210 × 135 m and 225 × 120m, respectively. The ground fracturing action reduces the spatial influence range of the high-level hard strata breakage. The area of the overlying strata that acts on the working face supports is denoted as S. According to the statistics, the area, S, after the breakage of KS4 and KS5 before and after KS5 is fractured is given in Table 2.

Table 2 The statistics of overburden S area

No	Items	KS4 breakage	KS5 breakage
1	KS5 unfractured	S_1— 4643.78	S_2— 6638.08
2	KS5 fractured	S_1′–3774.06	S_2′–1062.97
3	Ratio (S′/S)	81.3%	16.01%

It is easy to see from Table 2 that the ground fracturing causes the area, S, to decrease in KS4 and KS5 breakage, and the area, S, of the KS4 breakage is reduced to 81.3%. The ground fracturing has the most significant control effect on the mine pressure caused by KS5, and the area, S, of KS5 breakage is significantly reduced to 16.01%, which highly alleviates the strength of the mining pressure.

In summary, it can be seen that after KS5 is ground fractured, the broken structure of KS5 is changed, and the stable rock stratum structure of KS5 is no longer present. The rotation process of the KS5 structure is sluggish, which significantly reducing the pressure effect of KS5. In addition, after KS5 is fractured, the load strength of the underlying strata is increased, resulting in a decrease in the breaking span. However, KS5 does not rotate synchronously with the underlying strata, and so, it does not increase the pressure strength of the underlying strata. Contrastingly, the pressure strength of the underlying hard strata (i.e., KS4) decreases with the decrease in the breaking span.

4 Engineering application

The 8218 working face of the Tashan coal mine in the Datong mining area was selected as the test site. The geological conditions of 8218 working face is similar to that of 8101 working face. The 8218 working face is 230 m long, and the strike length is 2894 m. The thickness, burial depth, and inclination of the coal seam are 15 m to 22 m, 414.5 m to 632.1 m, and 2°, respectively. The mining method of top-coal caving is used. The coal seam is covered with multiple hard rock layers. The hard rock layers are mostly lithologically compact and medium-sized and coarse-grained sandstones. Particularly in the 110 m vertical distance from the coal seam, a 20-m-thick hard sandstone is formed. According to the above research, in extra-thick coal seam mining, when the ratio of the distance between the hard strata and coal seam to the coal seam thickness is between 5.3 and 7.3, the mine pressure of the hard strata breaking is the strongest. This is the main factor causing the strong mining pressure of the working face (Yu et al. 2019; Gao 2018), based on which 20-m-thick and hard rock formations are designated as the fractured target layers.

A horizontal well can realize multistage fracturing, for which the control range is wide and the fracturing effect is good. In view of the need to achieve high-efficiency control of high-level thick and hard rock layers, a horizontal well is adopted in this experiment.

4.1 Fracturing Process and Equipment

The horizontal fracturing well consists of a vertical section, deflecting section, and horizontal section. The position of the wellhead is 99 m away from the stop line of the working face, 105 m away from the return airway, and 125 m away from the intake airway. The horizontal section of the fracturing well extends parallel to the mining direction of the working face but opposite to the mining direction. The vertical section of the fracturing well adopts a three-level structure. The first level is drilled to 30 m with a Φ-444.5-mm drill bit, and a Φ-339.7 × 9.65-mm surface casing is inserted. The second level is drilled to 120 m with a Φ-311.5-mm drill bit, and a Φ-244.5×8.94-mm intermediate casing is inserted. The third level is drilled to 650 m with a Φ-216-mm drill bit, and a Φ-139.7×7.72-mm intermediate casing is inserted. The length of the deflecting section is 330 m, and the horizontal section is 200 m long. The relative positions of the fracturing well and working face and the fracturing well structure are shown in Fig. 8.

The area around the target fractured strata was perforated by drilling numerous small holes on the walls of the fracturing well. These allow the fracturing fluid to expand, thereby achieving the fracturing purpose. The target strata were designed to be fractured by three-stages in the horizontal section. To ensure the fracturing effect, the perforation density in the fractured zone is designed to be as high as 16 per meter. When the ground fracturing is performed, five pump trucks, one sand mixer, one instrument vehicle, five liquid tank trucks, and one sand tank truck are used. The reserve fracturing water is 2000 m^3. The ground fracturing site construction is shown in Fig. 9.

The maximum bursting pressure in the first stage is 12.46 MPa, and the total liquid volume is 470.9 m^3. The maximum bursting pressure in the second stage is 10MPa, and the total liquid is 549 m^3. The maximum bursting pressure in the third stage is 10.33 MPa, and the total liquid is 576.9 m^3.

4.2 Fracturing Effect Analysis

4.2.1 Crack propagation monitoring

The detectors were placed on the ground to monitor the microseismic wave signal during the fracturing process to describe the law of hydraulic crack propagation. Taking the fracturing well as the center, the detectors were arranged around the fracturing well, and the arrangement is shown in Fig. 10.

The positions of the detectors are listed in Table 3. The detectors were accurately positioned with high-precision GPS (GPS accuracy is not more than 3.0 m), and the ground depth of the detectors was not less than 30 cm.

Table 3 Coordinates of the detectors

	X	Y	Z	DX	DY	DZ
Wellhead	498150	4420432	1490			
A1	498064	4420648	1452	-86	216	-38
A2	498036	4420649	1446	-114	217	-44
A3	498004	4420655	1438	-146	223	-52
A4	497976	4420654	1434	-174	222	-56
A5	497954	4420656	1435	-196	224	-55
A6	497929	4420672	1438	-221	240	-52
A7	497896	4420677	1434	-254	245	-56
A8	497860	4420686	1429	-290	254	-61
B1	497971	4420500	1512	-179	68	22
B2	497963	4420514	1514	-187	82	24
B3	497807	4420575	1496	-343	143	6
B4	497830	4420585	1482	-320	153	-8
B5	497936	4420511	1479	-214	79	-11
B6	497922	4420557	1485	-228	125	-5
B7	497829	4420463	1523	-321	31	33
B8	497848	4420530	1492	-302	98	2
C1	498004	4420417	1545	-146	-15	55
C2	497973	4420414	1540	-177	-18	50
C3	497937	4420438	1540	-213	6	50
C4	497902	4420443	1520	-248	11	30
C5	497885	4420460	1521	-265	28	31
C6	497880	4420484	1519	-270	52	29
C7	497878	4420520	1488	-272	88	-2
C8	497775	4420466	1536	-375	34	46

After the first stage of fracturing, the crack propagation pattern was monitored, as shown in Fig. 11(a). As can be seen from Fig. 11(a), the crack propagation direction is NE90°, and the expansion lengths are 134 m and 62 m, respectively. After the second stage of fracturing, the crack propagation was monitored, as shown in Fig. 11(b). It can be seen from Fig. 11(b) that the crack propagation direction is NE55°, the crack spreads in two opposite directions, and the expansion lengths are 98 m and 118 m, respectively. The total length of the crack is 216 m. After the third stage of fracturing, the crack propagation was monitored, as shown in Fig. 11(c). It can be seen from the figure that the crack propagation direction is NE50°, and the cracks extend in two opposite directions. The expansion lengths are 118 m and 98 m, respectively, and the total crack length is 216 m.

The morphological characteristics of the cracks after fracturing thrice in the horizontal section are listed in Table 4. The fracturing crack extending in the horizontal direction is 216 m, which is longer than the working face length. The expansion direction is approximately perpendicular to the horizontal section of the fracturing well. The crack extending in the vertical direction is 50 m, and the crack expansion range is wide, completely covering the thickness range of the fractured target layer.

Table 4 Crack morphology statistics of the three stages

No	Stage	Crack length (m)		Crack height (m)		Propagation direction (°)
		left	right	upward	downward	
1	First stage	134	62	22	21	NE90
2	Second stage	98	118	24	26	NE55
3	Third stage	118	98	22	25	NE50

4.2.2 Ground pressure control effect

To monitor the deformation of the working face after the ground fracturing in the range of crack expansion, the hydraulic supports in the middle of the working face were selected to note the resistance of the working face in the normal mining section and fractured crack extension range. The roadway deformation monitoring points were also arranged at intervals of 10 m in the normal mining section and fractured crack extension area in the roadway, and were recorded as #1–#6, respectively, to monitor the deformation of the roadway, as shown in Fig. 12.

The roadway deformation and support resistance before and after the working face enters the ground fracturing control zone are shown in Fig. 13. The deformation characteristics of the roadway ahead of the working face at 20 m of each measuring point are shown in Fig. 13(a). The roadway deformation at #1 measuring point and #3 measuring point is large, which is mainly owing to the large mining thickness of the coal seam. The roadway deformation is significant in the advanced 20 m of the working face, and the extent of the roof-to-floor and two-side convergence is more than 1500mm. The bending of the single pillar is prominent. When the working face enters the ground fracturing control zone, the roadway deformation in advance is highly controlled. Taking #5 measuring point as an example, the roadway deformation is less than 300 mm, the single props do not exhibit any bending phenomenon, and the roadway maintenance is in excellent condition.

The characteristics of the support resistance before and after the working face enters the ground fracturing control zone are shown in Fig. 13(b). It can be clearly seen from the figure that the periodic roof weighting pace of the working face is in the range from 35 m to 55 m before the working face enters the ground fracturing control zone. Affected by the breakage and instability of the hard roofs, the compressive strength is up to 43 MPa, which has an obvious influence on the working face. When the working face is mined into the ground fracturing control zone, there are no obvious weighting step characteristics. The maximum strength of the supports is reduced to 30 MPa.

In summary, after the ground fracturing of the high-level hard and thick strata, the integrity and structural characteristics of the hard strata are destroyed, which reduces the energy intensity of the strata breakage. The surrounding rock failure and compressive strength of the supports are significantly controlled. It can be seen that the ground fracturing has a positive effect on ameliorating the stress environment of the stope, controlling the deformation of the surrounding rock, and reducing the strength of the mine pressure. This is a new and powerful approach to control the hard roofs in coal mining areas.

Conclusions

(1) The research shows that in the condition of extra-thick coal seam mining, the breaking and instability of thick and hard strata at a vertical distance of 100 m above the coal seam are the main reasons causing the presence of a strong ground pressure. The paper proposes to use the method of ground fracturing to weaken high-level hard roof and only employing clear water, which are economical and environmentally friendly and have a strong operability.

(2) The physical simulation studies show that the ground-fractured high-level hard strata action reduces the breakage steps and changes the structural characteristics of the strata. The breakage of the high-level hard strata is no longer a transient, high-speed, high-intensity process but a process of slow rotation, which reduces the strata breaking strength and mining pressure. The control effect of ground fracturing is remarkable.

(3) A horizontal fracturing well is used for the fracturing test on the site. The fracturing target layer is 20 m thick and 110 m vertically away from the coal seam. The fracturing process is performed in three stages. The microseismic monitoring shows that the horizontal extension length of the fracturing crack reaches 216 m, the height reaches 50 m, and the expansion range is wide. The ground fracturing releases the strata stress concentration and changes the strata structure and its mining pressure action. After the ground fracturing, the roadway deformation and support resistance of the 8218 working face are highly controlled, and the ground fracturing control effect is remarkable.

(4) The successful test of the horizontal fracturing well shows that the control range and fracturing effect of the ground fracturing are remarkable, which provides a new approach for the control of the high-level hard and thick strata in coal mines and is of tremendous significance. In addition, the horizontal fracturing well can achieve multistage fracturing with a strong controllability and operability and has broad application prospects.

Declarations

Availability of data and materials

The data and material are transparency in the paper.

Competing interests

None.

Funding

This work was supported by the State Key Research Development Program of China [grant number 2018YFC0604500]; the China Postdoctoral Science Foundation [grant number 2019M651080]; applied basic research project of Shanxi Province [grant number 201901D211030], and Scientific, Technological Innovation Programs of Higher Education Institutions in Shanxi (STIP) [grant number 2019L0208], and Major Program in Shanxi Province [grant number 20191101015].

Authors' contributions

Rui Gao designed the study, participated in data analysis, carried out sequence alignments; Tiejun Kuang participated in the design of the study and drafted the manuscript; Yanqun Zhang carried out the physical simulation and analysed the data; Wenyang Zhang and Chunyang Quan helped draft the manuscript and collected the field measurement data. All authors gave final approval for publication.

References

1. Bednarek L, Majcherczyk T (2020) An analysis of rock mass characteristics which influence the choice of support. Geomech Eng 21(4): 371-377.
2. Gao R (2018) The Mechanism of ground pressure induced by the breakage of far-field hard strata and the control technology of ground fracturing. Dissertation, China University of Mining and Technology.
3. Ge ZL, Mei XD, Lu YY, Tang JR, Xia BW (2015) Optimization and application of sealing material and sealing length for hydraulic fracturing borehole in underground coal mines. Arab J Geosci 8: 3477.
4. Guo WB, Liu CY, Wu FF, Yang PJ, Wu SF (2014) Analyses of support crushing accidents and support working resistance in large mining height workface with hard roof. Journal of China Coal Society 39(07): 1212-1219.
5. Ju JF, Xu JL (2013) Structural characteristics of key strata and strata behavior of a fully mechanized longwall face with 7.0 m height chocks. Int J Rock Mech Min Sci 58: 46-54.
6. Lan YW, Gao R, Yu B, Meng B (2018) In situ studies on the characteristics of strata structures and behaviors in mining of a thick coal seam with hard roofs. Energies 11(9): 2470.
7. Li HM, Jiang DJ, Li DY (2014) Analysis of ground pressure and roof movement in fully-mechanized top coal caving with large mining height in ultra-thick seam. Journal of China Coal Society 39(10):1956-1960.
8. Li Z, Xu JL, Ju JF, Zhu WB, Xu JM (2018) The effects of the rotational speed of voussoir beam structures formed by key strata on the ground pressure of stopes. Int J Rock Mech Min Sci 108: 67-79.
9. Lu YY, Cheng L, Ge ZL, Xia BW, Li Q, Chen JF (2015) Analysis on the initial cracking parameters of cross-measure hydraulic fracture in underground coal mines. Energies 8(7): 6977-6994.
10. Lu YY, Gong T, Xia BW, Yu B, Huang F (2018) Target stratum determination of surface hydraulic fracturing for far-field hard roof control in underground extra-thick coal extraction: a case study. Rock Mech Rock Eng 52(8): 2725-2740. 10.1007/s00603-018-1616-9.
11. Ning JG, Wang J, Jiang LS, Jiang N, Liu XS, Jiang JQ (2017) Fracture analysis of double-layer hard and thick roof and the controlling effect on strata behavior: A case study. Eng Fail Anal 81: 117-134.
12. Tan YL, Liu XS, Shen B (2018) New approaches to testing and evaluating the impact capability of coal seam with hard roof and/or floor in coal mines. Geomechanics and Engineering 14(4): 367-376.
13. Wang J, Ning JG, Qiu PQ (2019) Microseismic monitoring and its precursory parameter of hard roof collapse in longwall faces: A case study. Geomechanics and Engineering 17(4): 375-383.
14. Xia BW, Jia JL, Yu B, Zhang X, Li XL (2017) Coupling effects of coal pillars of thick coal seams in large-space stopes and hard stratum on mine pressure. International Journal of Mining Science and Technology 27: 965-972.
15. Xie JL, Xu JL (2017) Effect of key stratum on the mining abutment pressure of a coal seam. Geosci J 21(2): 267-276.
16. Yang JX, Liu CY, Yu B. (2015) Mechanism of complex mine pressure manifestation on coal mining work faces and analysis on the instability condition of roof blocks. Acta Geodyn Geomater 12(1): 101-108.
17. Yang JX, Liu CY, Yu B. (2017) Application of confined blasting in water-filled deep holes to control strong rock pressure in hard rock mines. Energies 10: 1874.
18. Yang JX, Liu CY (2017) Experimental study and engineering practice of pressured water coupling blasting. Shock Vib 548459810.1155/2017/5484598.
19. Yan H, Zhang JX, Zhang S, Zhou N (2018) Physical modeling of the controlled shaft deformation law during the solid backfill mining of ultra-close coal seams. B Eng Geol Environ 2: 1-14.
20. Yu B (2016) Behaviors of overlying strata in extra-thick coal seams using top-coal caving method. Journal of Rock Mechanics and Geotechnical Engineering 8: 238-247.
21. Yu B, Duan HF (2014) Study of roof control by hydraulic fracturing in full-mechanized caving mining with high strength in extra-thick coal layer. Chinese Journal of Rock Mechanics and Engineering 33(4): 778-785.
22. Yu B, Gao R, Kuang TJ, Huo BJ, Meng XB (2019) Engineering study on fracturing high-level hard rock strata by ground hydraulic action. Tunn Undergr Sp Tech 86: 156-164.
23. Yu B, Zhao J, Kuang TJ, Meng XB (2015) In situ investigations into overburden failures of a super-thick coal seam for longwall top coal caving. Int J Rock Mech Min Sci 78: 155-162.

24. Yu B, Zhao J, Xiao HT (2017)Case study on overburden fracturing during longwall top coal caving using microseismic monitoring. Rock Mech Rock Eng 50: 507-511.
25. Zhang HW, Zhu ZJ, Huo LJ, Chen Y, Huo BJ (2014) Overburden failure height of superhigh seam by fully mechanized caving method. Journal of China Coal Society, 39(5): 816-821.

Figures

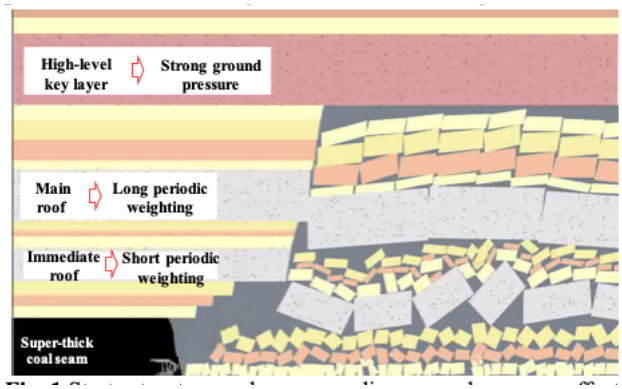

Figure 1

Strata structure and corresponding ground pressure effect

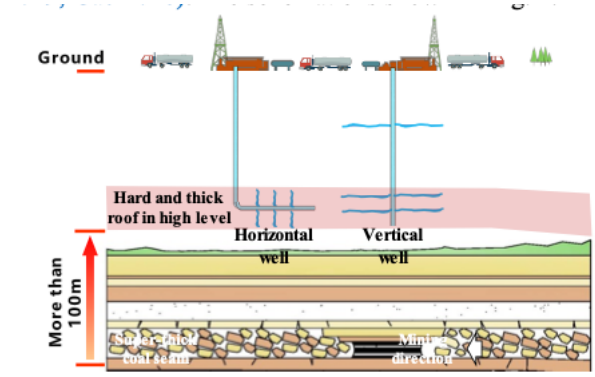

Figure 2

Ground hydraulic fracturing of high-level hard roofs

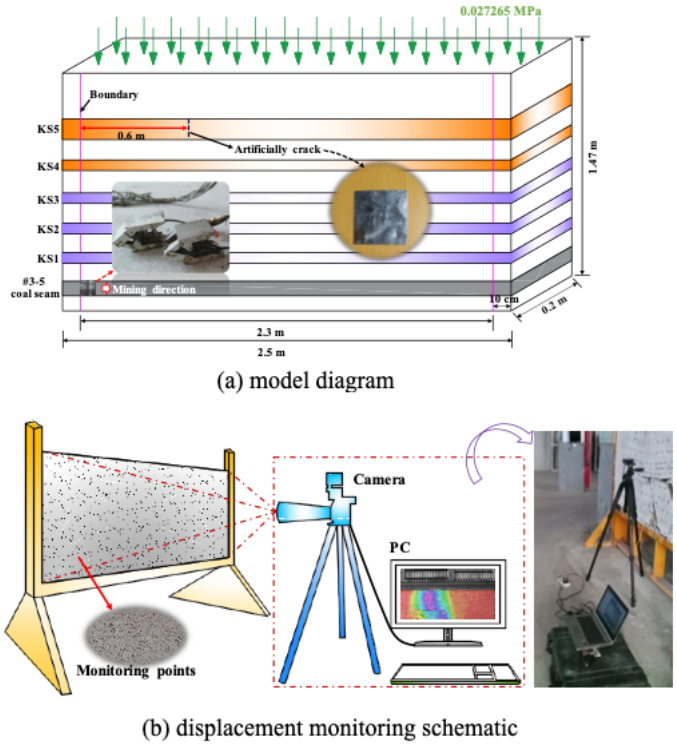

Figure 3

Physical model layering and monitoring scheme

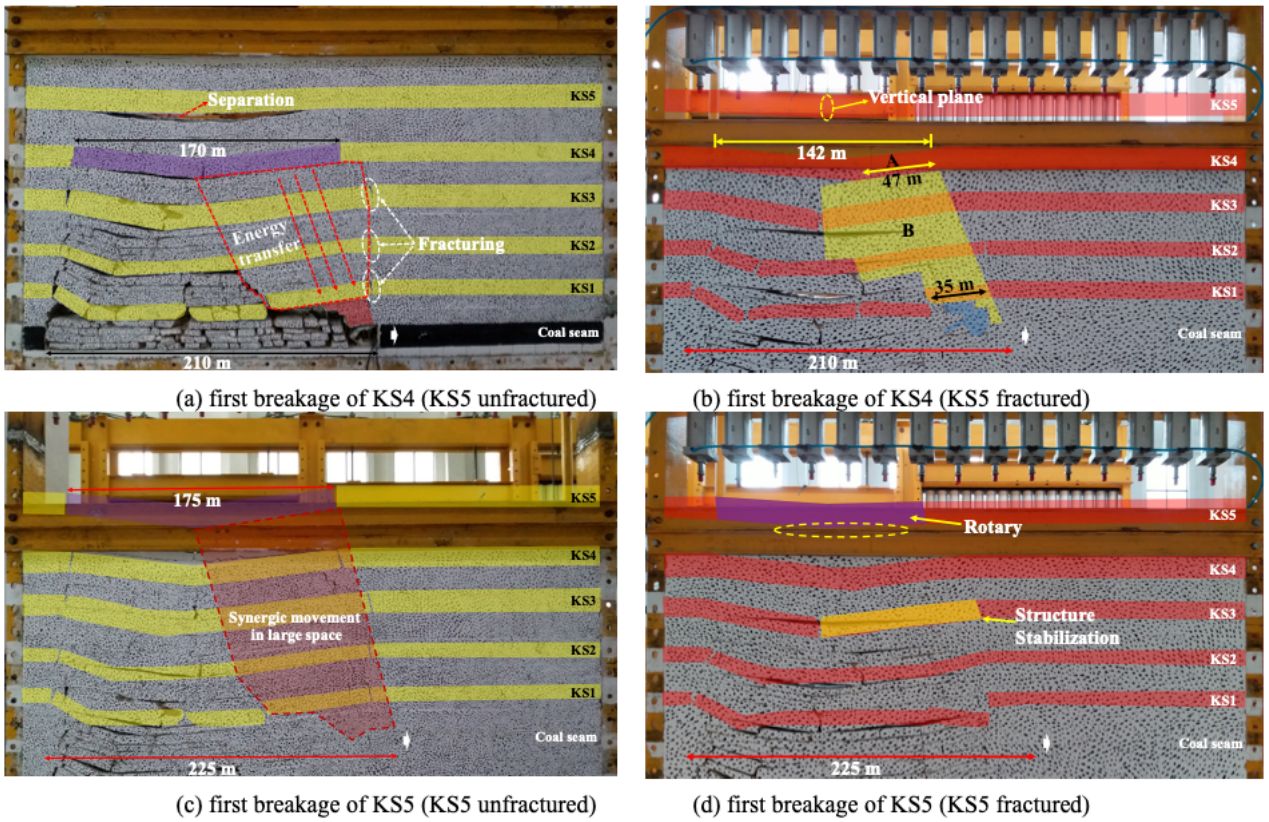

Figure 4

The characteristics of overburden breaking

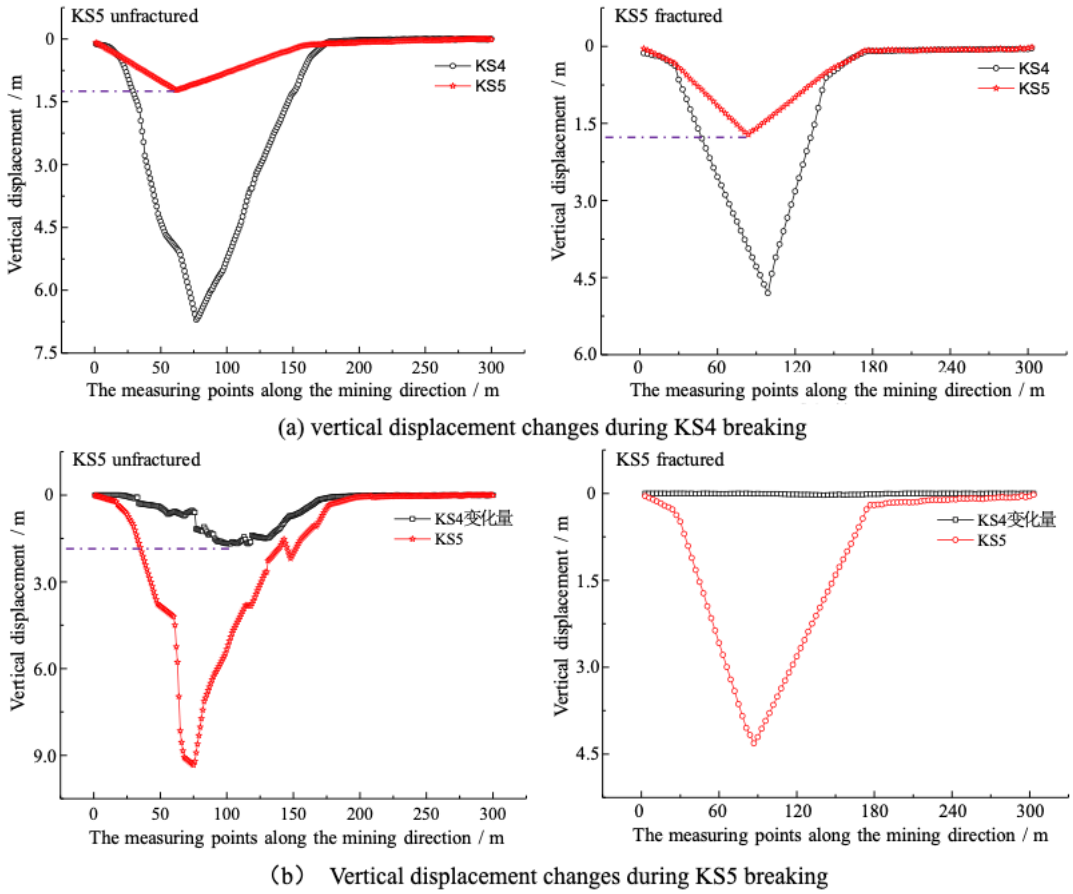

Figure 5

Vertical displacement caused by the KS5 fracturing

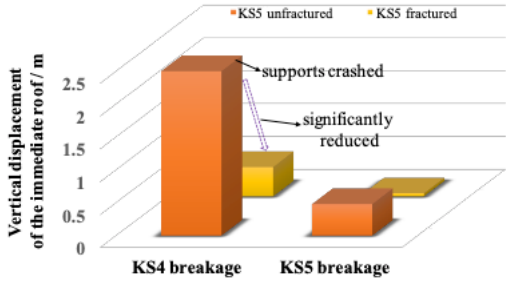

Figure 6

Comparison of the displacement of the immediate roof during KS4 and KS5 breaking

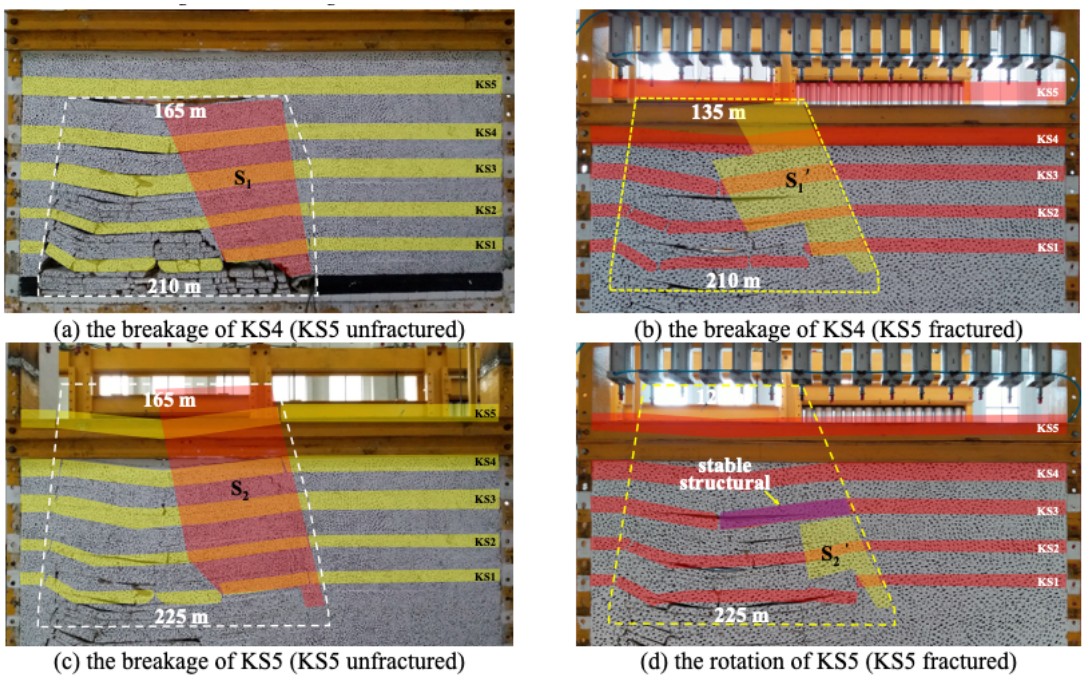

(a) the breakage of KS4 (KS5 unfractured)

(b) the breakage of KS4 (KS5 fractured)

(c) the breakage of KS5 (KS5 unfractured)

(d) the rotation of KS5 (KS5 fractured)

Figure 7

Overburden space structure of the breakage of KS4 and KS5

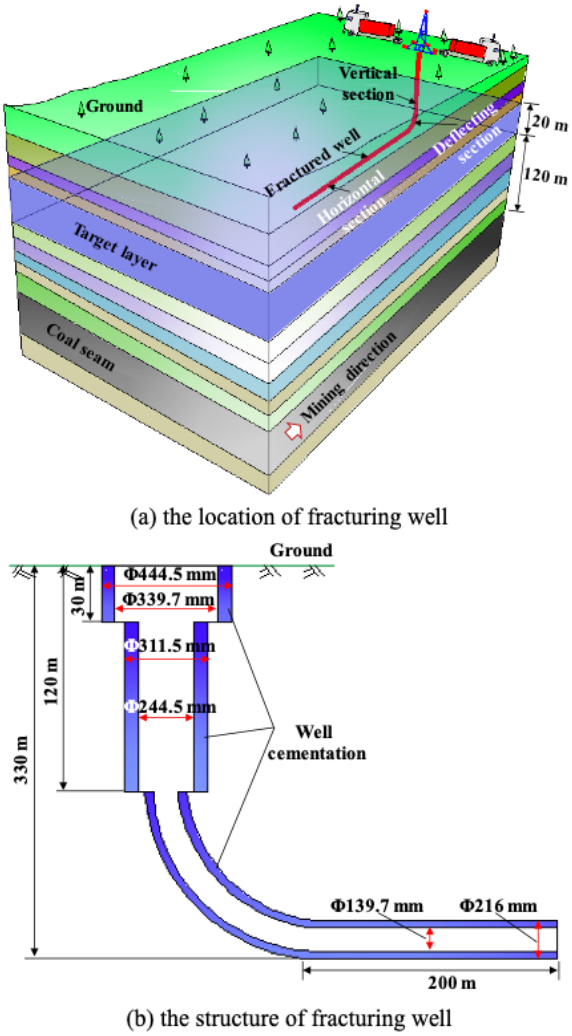

(a) the location of fracturing well

(b) the structure of fracturing well

Figure 8

Structural representation of the hydraulic fractured well

Figure 9

Construction site layout of the ground fracturing

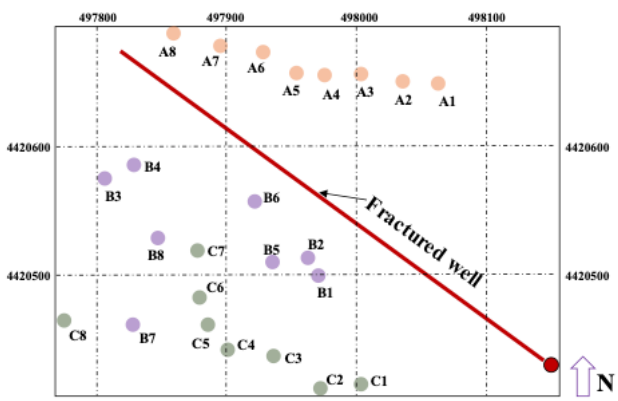

Figure 10

Position layout of the detectors

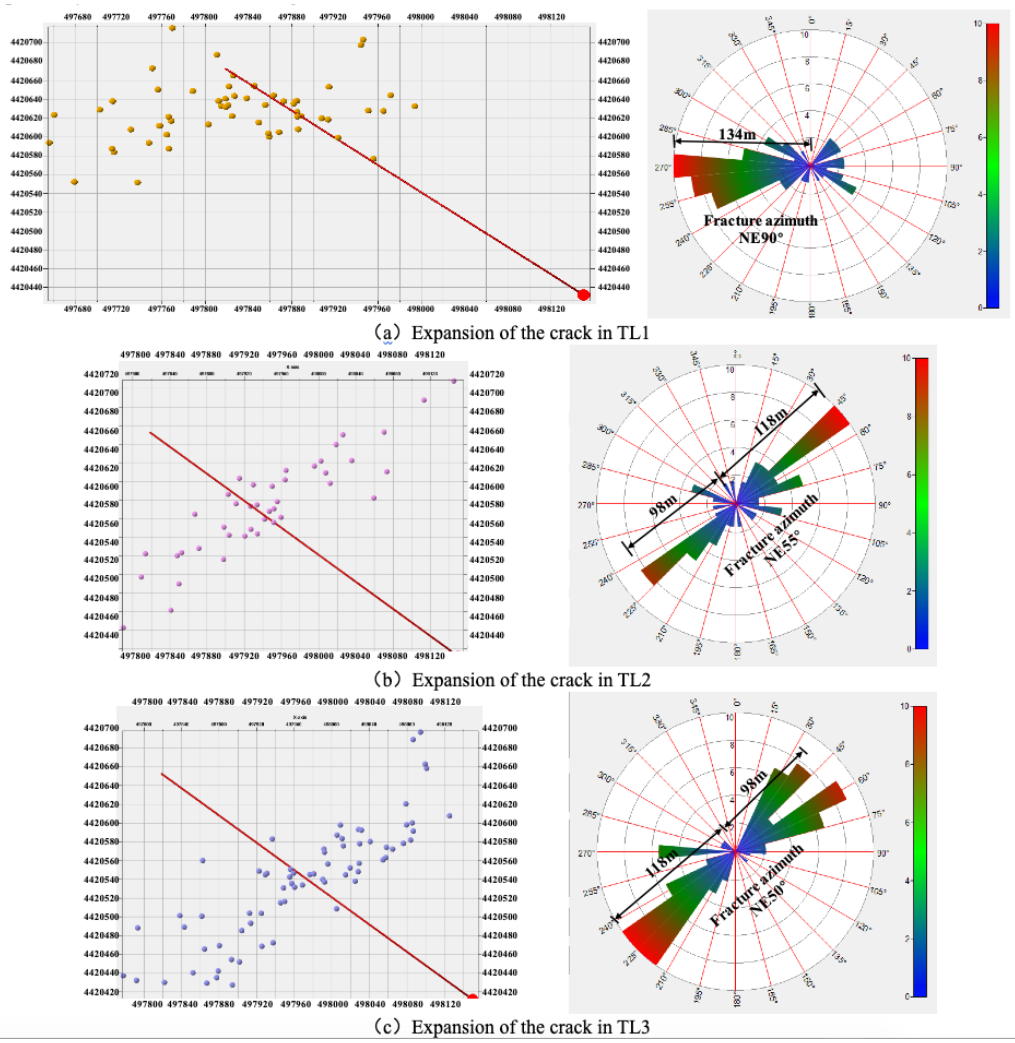

Figure 11

The expansion of crack in the three times fracturing

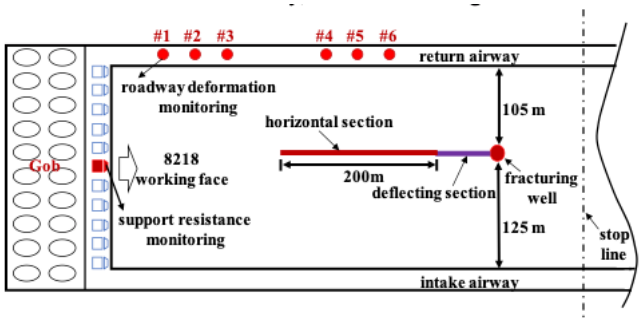

Figure 12

Ground pressure monitor layout

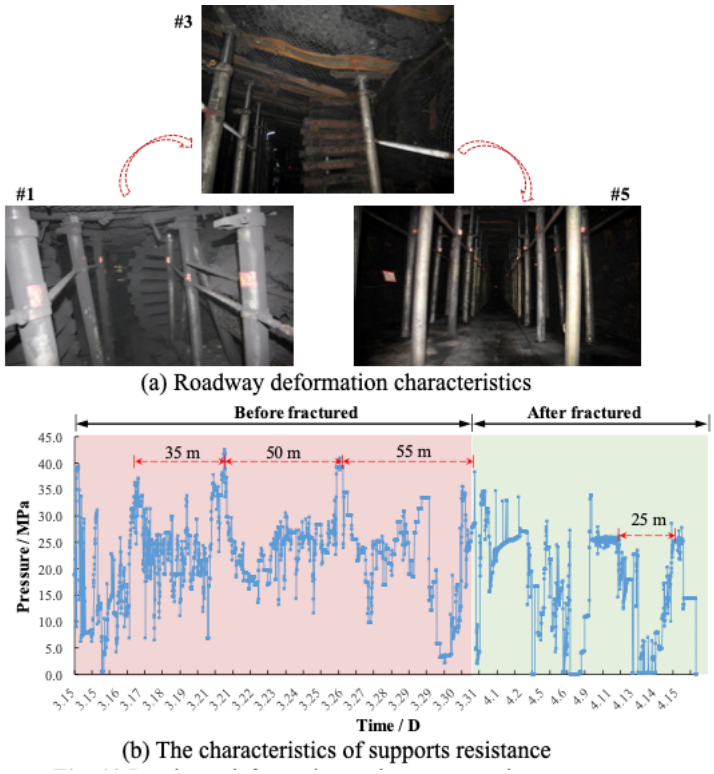

Figure 13

Roadway deformation and supports resistance influenced by the ground fracturing